Nuclear Engineering and Design 416 (2024) 112815

Contents lists available at ScienceDirect

Nuclear Engineering and Design

journal homepage: www.elsevier.com/locate/nucengdes

The influence of droplet breakup model on the prediction of reactor core parameters during reflood conditions

Omar S. Al-Yahia [a,*], Matthew Bernard [b], Ivor Clifford [a], Gregory Perret [a], Stephen Bajorek [b], Hakim Ferroukhi [a]

[a] Laboratory for Reactor Physics and Thermal-Hydraulics (LRT), Paul Scherrer Institut, 5232 Villigen PSI, Switzerland
[b] U.S. Nuclear Regulatory Commission, Washington, DC 20555-0001, USA

ARTICLE INFO

Keywords:
TRACE
Droplet entrainment
Reflood
Droplet field
Spacer grid

ABSTRACT

During reflood conditions, spacer grids affect the complex flow dynamics inside the reactor core. They can breakup the dispersed droplets, thereby significantly reducing their diameters. This process enhances local heat and mass interfacial transfer, consequently reducing the peak cladding temperature (PCT). Therefore, accurately predicting droplet transport and size within a reactor core is very important for reactor safety analysis. Recently, the US. NRC TRACE code has been modified by extending its governing equations to incorporate a three-field approach that captures the dynamic behavior of droplet entrainment, transport, and their interactions with structures within the reactor core. The new TRACE (v5.0 patch 8) three-field framework incorporates droplet models accounting for entrainment from liquid pools, liquid films on vertical surfaces, and droplet breakup. This paper focuses on the influence of the spacer grid droplet breakup model on the behavior of reactor core during reflood transient. The selected droplet breakup model effectively captures the enhancement in interfacial heat transfer observed in experimental data. We evaluate the influence of the droplet breakup model on the three-field version of TRACE by comparing it to recent Rod Bundle Heat Transfer (RBHT) experiments. These experiments had previously indicated that TRACE tended to overpredict the PCT for various initial and boundary conditions. Subsequently, we conducted a detailed comparison between TRACE v5.0 patch 7 and the three-field TRACE (v5.0 patch 8) with and without the spacer grid droplet breakup model. Our findings demonstrate a significant improvement in predictive accuracy with the new breakup model compared to the base capability of TRACE v5.0 patch 7. This improvement results in more accurate predictions of PCTs and quenching times for the assessed conditions.

1. Introduction

Many engineering systems experience scenarios involving the flow of two phases, such as heat exchangers, abnormal transients in pressurized water reactors (PWRs), and both normal and abnormal operations in boiling water reactors (BWRs). In the event of a postulated loss of coolant accident (LOCA) in light water reactors (LWRs), subcooled water is injected into the reactor core through the emergency core cooling system (ECCS). This is done to eliminate the decay heat and, consequently, maintain the peak cladding temperature (PCT) below the regulatory limit of 1478 K (IAEA, 2003). Following the water injection, a quenching process starts at the lower part of the reactor core and gradually progresses upwards to cool the reactor core. As a result, the upper region of the reactor core is expected to undergo a dispersed flow film boiling regime (DFFB). Meanwhile the PCT will continue to rise until adequate two-phase flow cooling is achieved. Eventually, the temperature will decrease until the entire reactor core is completely quenched (Jin et al., 2019). The increase in the PCT in the post-dryout regime is a significant safety concern as it can lead to a severe deterioration in heat transfer and result in the degradation of reactor components. Therefore, accurately estimating the mass and heat transfer involved in the DFFB regime is crucial. To enhance the precision of transient behavior calculations in nuclear power plants, thermal hydraulic system analysis codes like US-NRC TRACE are continuously improved (U.S.NRC, 2022). These enhancements involve solving the three field equations (Bernard and Bajorek, 2023), utilizing advanced numerical solving techniques, and selecting correlations and closure

* Corresponding author.
E-mail addresses: omar.alyahia@psi.ch (O.S. Al-Yahia), matthew.bernard@nrc.gov (M. Bernard), ivor.clifford@psi.ch (I. Clifford), gregory.perret@psi.ch (G. Perret), stephen.bajorek@nrc.gov (S. Bajorek), hakim.ferroukhi@psi.ch (H. Ferroukhi).

https://doi.org/10.1016/j.nucengdes.2023.112815
Received 3 October 2023; Received in revised form 23 November 2023; Accepted 30 November 2023

Nomenclature

Abbreviations and Acronyms

BWR	Boiling Water Reactor
DFFB	Dispersed Flow Film Boiling
ECCS	Emergency Core Cooling System
LB-	Large Break
LOCA	Loss of Coolant Accident
MFB	Minimum Film Boiling
PCT	Peak Cladding Temperature
PWR	Pressurized Water Reactor
RBHT	Rod Bundle Heat Transfer
d_o	Incoming droplet diameter [m]
$d_{s,32}$	Sauter mean diameter [m]
k	Kinetic energy fraction
$\dot{m}$	Mass flow rate
Nu_f	Nusselt number for interfacial convective heat transfer
Pr_f	Liquid Prandtl number
Re	Reynolds number
U_d	Incoming droplet velocity
We_d	Weber number of the incoming droplet
Y	The dimensionless radiation number

Greek

ε	Blockage ratio
γ	The liquid mass loss coefficient due to the evaporation of the small droplets
n_l	The number of new generated large droplets
n_s	The number of new generated small droplets
ρ	Density
σ	Surface Tension

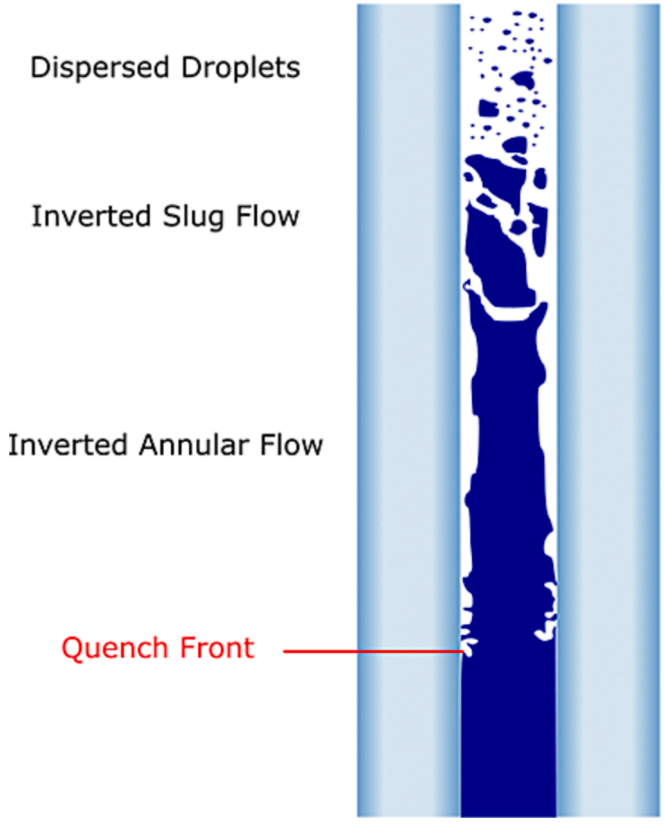

Fig. 1. Core reflood flow regimes.

modules associated with complex two-phase phenomena. The accuracy of code predictions is heavily influenced by the complexity of thermal hydraulic phenomena and geometric parameters. For instance, during a reflood transient in a nuclear reactor, all heat transfer and flow regimes are expected to occur within the heated tube bundle in the core region (Choi and No, 2012), as shown in Fig. 1. This can reduce the accuracy of predicting PCT and/or quenching times during the reflood phase, particularly in the presence of spacer grids. Hence, it is crucial to have a comprehensive understanding of the thermal–hydraulic response during the reflood phase of an accident to ensure that the cladding temperature remains below the acceptable safety limit (Cheung and Bajorek, 2011). The PCT is observed in the dispersed flow boiling regime, where liquid

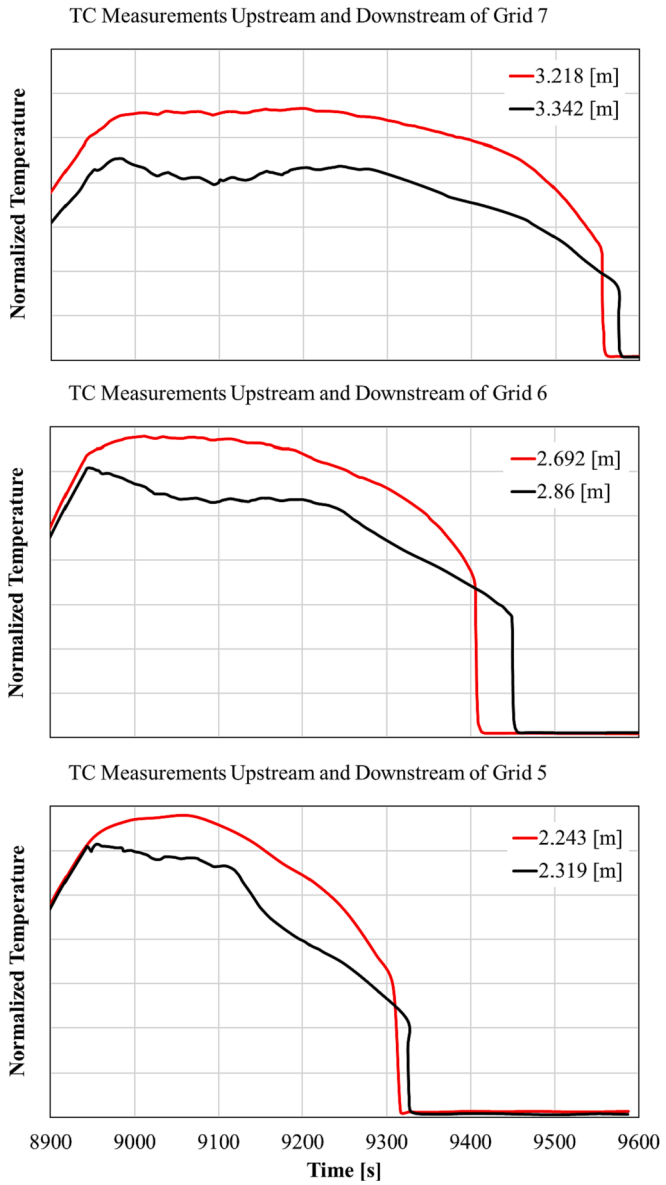

Fig. 2. The effect of spacer grid on the rod surface temperature of RBHT test 9021.

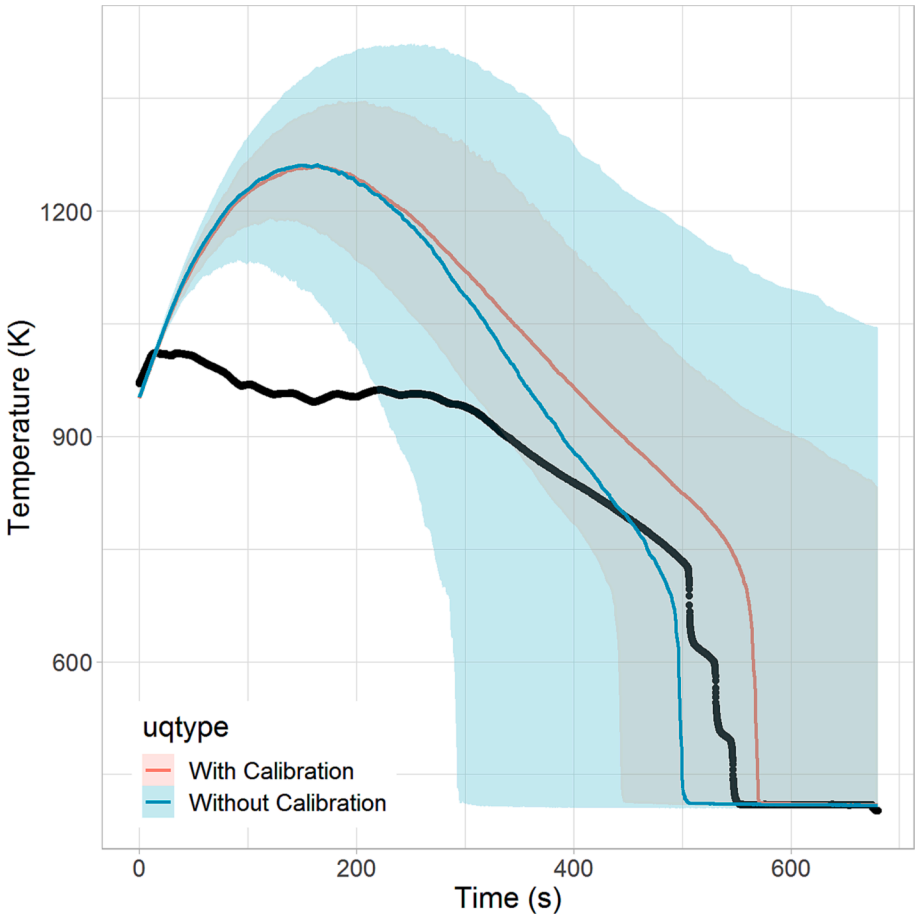

Fig. 3. Rod surface temperature for test 9021 of RBHT at 2.9 m elevation with uncertainty bands (95 % confidence intervals).

droplets are dispersed within the continuous vapor flow area. These dispersed droplets have a substantial surface area-to-volume ratio, facilitating significant interfacial areas for heat and mass transfer. This, in turn, leads to a reduction in the PCT. The improvement in the cooling rate is directly proportional to the size of the droplets, which determines the interfacial heat transfer area between the dispersed droplets and the continuous vapor (Cheung and Bajorek, 2011).

The Thermal-Hydraulic System Analysis Code, TRACE (U.S.NRC, 2022), evaluated by the U.S. Nuclear Regulatory Commission, serves as a tool for delivering best-estimate predictions concerning loss of coolant accidents (LOCAs), operational transients, and various accident scenarios in pressurized and boiling light water nuclear reactor designs. The analysis of these transients requires modeling a wide spectrum of physical phenomena, involving scenarios ranging from subcooled, single-phase liquid conditions to superheated steam. TRACE employs a simplified version of the two-fluid model (Ishii and Hibiki, 2010), containing six equations, each devoted to continuity, momentum, and energy equations for gas and liquid phases. Nevertheless, when dealing with the complexities of the reflood transient, the accuracy of predicting thermal hydraulic parameters moderates. Within the TRACE code, there exist specific models designed for estimating thermal hydraulic phenomena during the reflood transient (U.S.NRC, 2022). However, during the OECD/NEA RBHT project, numerous thermal hydraulic codes, TRACE included, exhibited an overestimation of rod surface temperatures and divergent predictions of the quench front within the rod bundle, in contrast to experimental outcomes (OECD/NEA, 2022). Similar observations were made in simulations of ABB Atom and FLECHT-SEASET reflooding tests (Choi and No, 2010; Koszela, 2003). Consequently, an extensive examination of the RBHT experimental data revealed that the spacer grid exerts a significant influence on heat and mass transfer throughout the rod bundle. As illustrated in Fig. 2, temperatures downstream of the spacer grids are lower than those upstream, although quenching is delayed downstream. TRACE incorporates specialized models to account for spacer grid effects, including pressure drop increases, enhancements in single-phase heat transfer, and a spacer grid rewet model (U.S.NRC, 2022). However, despite the inclusion of these models, TRACE failed to replicate the observed trend.

Throughout the RBHT project, TRACE simulations were conducted using multiple code versions, with an evaluation of the sensitivity of model parameters playing a significant role in reflood experiments (Perret et al., 2019). 27 uncertain parameters were considered, which are derived from the physical models of the Dispersed Flow Film Boiling (DFFB) and Inverted Annular Film Boiling (IAFB) flow regimes, the models related to the spacer grid, transition boiling, and minimum film boiling. More details about the uncertainty analysis can be found in (Perret et al., 2019). Fig. 3 provides an example of rod surface temperature predictions made with TRACE. The figure shows the Rod surface temperature for test 9021 of RBHT at 2.9 m elevation with uncertainty bands (95 % confidence intervals) resulting from the model parameter uncertainty. Uncertainty bands are derived using model parameter uncertainty that are conservative (labelled without calibration) and that have been calibrated against similar experiments (labelled with calibration). Even when the probability distribution of model parameters was conservatively assessed, i.e., without calibration, the uncertainty bands did not encompass the experimental temperature profile. Consequently, the TRACE models prove inadequate in capturing the physics exhibited in such reflood experiments.

In commercial nuclear reactors like BWRs and PWRs, spacer grids are employed within the fuel rod assemblies to maintain a consistent gap between the rods. These grids serve the dual purpose of preventing

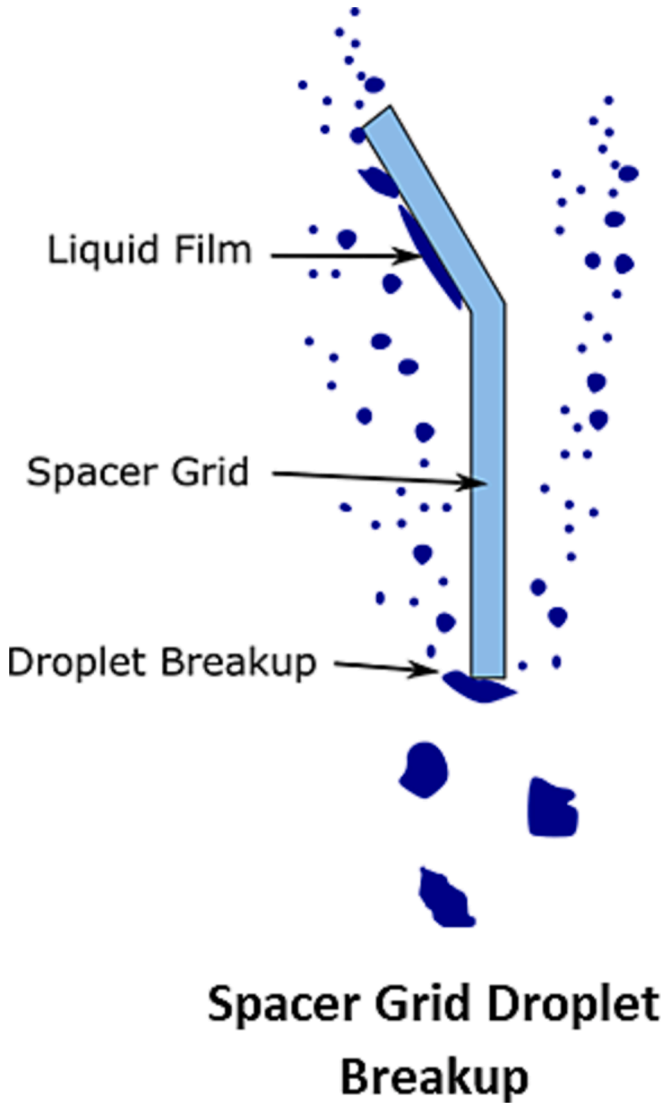

Fig. 4. Schematic diagram of droplet breakup at spacer grid.

damage caused by vibrations from fluid flow and ensuring a clear pathway for the flow. To further enhance their performance, mixing vanes are incorporated into these spacer grids. These vanes generate cross-flows and vortices that enhance turbulence and local heat transfer (Chun and Oh, 1998). An interesting effect of these spacer grids is their ability to shatter or split incoming dispersed droplets, significantly reducing their size. This reduction in droplet size results in a larger interfacial area, leading to increased heat and mass transfer at the local level. Therefore, it effectively lowers the peak cladding temperature (PCT). In experiments of reflood test on a 6x6 heated rod bundle, Sugimoto and Urao (Sugimoto and Muraov, 1984) observed substantial droplet breakup when droplets collided with the grid spacer straps. Notably, the downstream droplet diameter decreased as the grid blockage ratio increased. The spacer grid's effectiveness in breaking down incoming droplets is further enhanced when dealing with larger droplet diameters (Lee et al., 1983; S. L. Lee et al., 1984). Consequently, significant droplet breakup can occur when droplets with a high Weber number (determined by factors such as droplet diameter, density, velocity, and surface tension) collide with the spacer grid straps. This phenomenon gives rise to the creation of new droplets with smaller Sauter diameters and higher number densities. Consequently, it increases the interfacial heat transfer area downstream of the spacer grid and accelerates the flow. Simultaneously, it cools the rods downstream of the spacer grid through the rapid evaporation of the fragmented droplets (Chiou et al., 1982).

Over the past few decades, there has been extensive research into the interfacial heat and mass transfer behavior within a droplet field entrained in continuous vapor field. When spacer grids are introduced into this scenario, the droplets encounter the spacer grid's dry and wet surfaces at varying angles (Jin et al., 2019). Several researchers have shown interest in studying how droplets break apart upon colliding with spacer grids and how this phenomenon affects the PCT during the reflood phase (Cheung and Bajorek, 2011; Nithianandan et al., 1995). In 1966, Wachters and Westerling (Wachters and Westerling, 1966) conducted an experimental study to investigate the impact of the Weber number on droplet breakup. They discovered that droplet breakup occurred when the Weber number of the incoming droplets exceeded 80. The Weber number represents the ratio of droplet inertia to surface tension, highlighting the significant influence of incoming droplet velocity on droplet heat transfer (Pederson, 1967). Subsequently, Hamdan et al. (Hamdan et al., 2015) conducted their own experimental study, examining droplet behavior above the minimum film boiling (MFB) temperature. Their findings revealed that droplets did not break apart when the Weber number was below 30. However, for larger Weber numbers, incoming droplets fragmented into several micro-sized droplets and a larger droplet with a diameter smaller than the original incoming droplet.

To estimate the shattered droplet diameter, several empirical correlations have been developed, taking into account the Weber number, spacer grid blockage ratio (Paik et al., 1985), and the ratio of incoming droplet diameter to spacer grid strip thickness (Yao et al., 1988). In 1977, Paddock (Paddock, 1977) utilized photography to observe droplet behavior and noted an increase in the number of droplets downstream of the spacer grid due to droplet breakup. Rane and Yao (Rane and Yao, 1981) demonstrated that in a dispersed two-phase flow regime, droplets could function as a distributed heat sink within the continuous vapor phase region.Senda (Senda, 1982) searched into the interaction of droplets with heated flat plates and observed that high Weber numbers could cause droplets to flatten into liquid sheets before fragmenting into smaller droplets. In 1998, Koszela (Koszela, 1998) conducted an experimental study using a 3x3 rod bundle to investigate the influence of spacer grid design on reflood heat transfer. He found that the use of mixing vane spacer grids significantly reduced the PCT at low reflood rates but decreased heat transfer in the post-critical heat flux (CHF) regime at high reflood rates. Similar findings regarding the effects of spacer grid types on heat transfer enhancement in a rod bundle were observed experimentally by Cho et al. (Cho et al., 2007) and numerically by In et al. (In et al., 2008).

Droplet breakup within the Dispersed Flow Film Boiling (DFFB) regime plays a crucial role in enhancing the cooling effectiveness during the reflood process. To precisely assess this cooling enhancement, it becomes essential to determine the ratio of Sauter mean diameters of droplets downstream and upstream of the grid. Cheung and Bajorek (Cheung and Bajorek, 2011) formulated a model to predict the Sauter mean diameter of the newly formed droplets downstream of the wet spacer grid. Recently, Jin et al. (Jin et al., 2019) extended the research initiated by Cheung and Bajorek (Cheung and Bajorek, 2011) to predict droplet breakup for the dry spacer grid. They established a relationship between the Sauter mean diameter ratio and the governing parameters of the dispersed flow-grid spacer system, validating their model against RBHT experimental data.

Consequently, in the present investigation, the droplet breakup models by Cheung and Bajorek (Cheung and Bajorek, 2011) and Jin et al. (Jin et al., 2019) for wet and dry spacer grids, respectively, have been implemented into the nuclear thermal hydraulic system analysis code TRACE. This implementation within the TRACE code aims to provide more accurate predictions for reflood peak clad temperatures (PCTs) and quenching times. These spacer grid droplet breakup models are rooted in energy and mass balance considerations and the droplet

Table 1
Definition of droplet breakup model parameters.

Breakup model parameters	Definition
$k = 2.164We_d^{-0.442}$	Kinetic energy fraction of the incoming droplet that is converted to surface energy of the new generated droplets
$n_s = \frac{n_l}{C}\frac{d_l^3}{d_o^3}\frac{d_o^3}{d_s^3}$	The number of new generated small droplets
$n_l = 1\ 2$	The number of new generated large droplets
$\frac{d_s}{d_o} = \left[\left(\frac{kWe_o}{12} + 1 - n_l\frac{d_l^2}{d_0^2}\right) \Big/ \left(\frac{n_l}{C}\frac{d_l^3}{d_o^3}\right)\right]^{-1}$	The ratio of new small group Sauter diameter to the incoming droplet Sauter diameter
$\frac{d_l}{d_o} = \left(\frac{C}{(1+C)n_l}\right)\frac{1}{3}$	The ratio of new large group Sauter diameter to the incoming droplet Sauter diameter
$C = \frac{F_l}{1-F_l}$	The volume ratio of the large droplet group to small droplet group
$F_{l=}\left(0.0042\left(\frac{d_o}{W}\right) - 0.0386\right)\ln We_d + 1.04$	The volume fraction of large droplet groups to the original droplet volume
$\gamma = 0.55\left(\left(\frac{Nu_f Ja_f}{Pr_f Re_d} + Y\right)\left(\frac{L}{d_s}\right)\right)^{0.27}$	The liquid mass loss coefficient due to the evaporation of the small droplets
$Y = \frac{\varepsilon_r \sigma\left(T_w^4 - T_d^4\right)}{h_{fg}\rho_d u_d}$	The dimensionless radiation number
$Nu_f = \left(2 + 0.57Re_v^{0.5}Pr_f^{0.33}\right)\left(1 + B_f\right)^{-0.7}$	Nusselt number for interfacial convective heat transfer
$Re_v = \frac{\rho_v u_r d_s}{\mu_v}$	Vapor Reynolds number
$Pr_f = \frac{C_p \mu_f}{k_f}$	Liquid Prandtl number
$B_f = Ja_f = \frac{C_p(T_v - T_d)}{h_{fg}}$	Mass transfer number
$Re_d = \frac{\rho_d u_d d_s}{\mu_v}$	Droplet Reynolds number

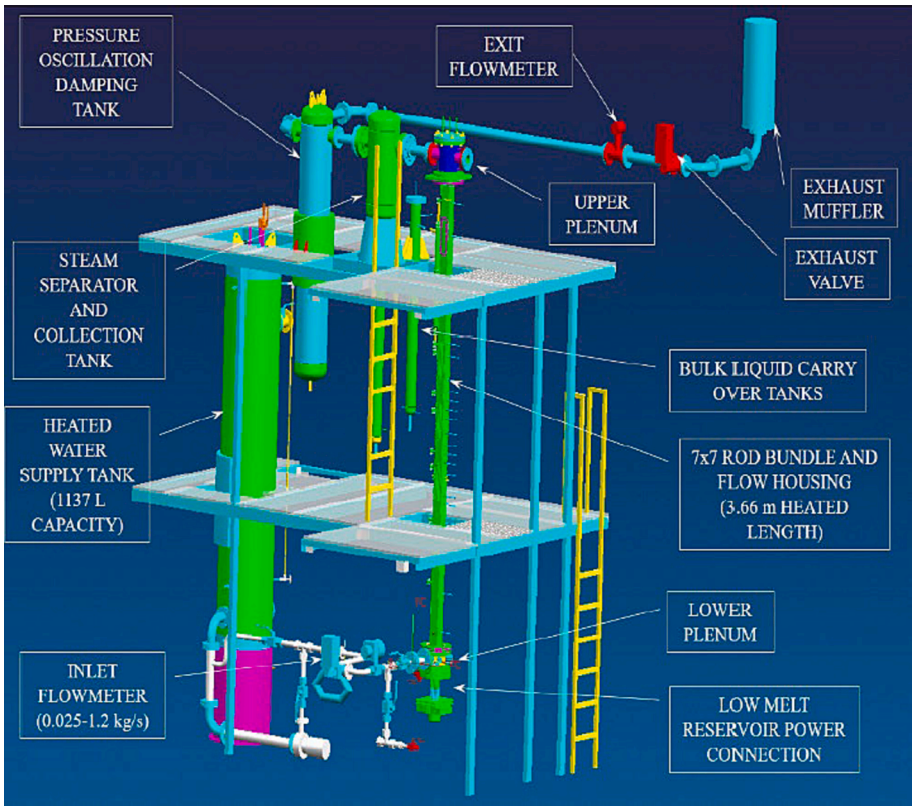

Fig. 5. RBHT testing facility (Lowery et al., 2023).

Weber number, and they are integrated into the newly developed three-field version of the U.S. Nuclear Regulatory Commission's TRACE code (Bernard and Bajorek, 2023). To evaluate the impact of the droplet breakup model on the three-field TRACE version, comparisons are made against recent RBHT experiments. In prior studies, TRACE had been shown to overpredict rod surface temperature and PCT under various initial and boundary conditions. Additionally, a sensitivity analysis is conducted to investigate the influence of time steps on predicting rod surface temperature during the reflood process.

Table 2
Boundary conditions for OECD-RBHT tests.

Test	Reflood rate (cm/s)	Reflood inlet subcooling (K)	Bundle power (kW)
9005	5	14	144
9011	Step (8, 5, 3, 1.2)	26	144
9012	Varying (±2.5)	9	144
9014	15	80	252
9015	15	12	252
9021	2.5	10	144
9026	2.5	79	144
9027	2.5	32	144
9029	2.5	48	222 (Decay)
9037	5	11	144
9043	0.5	2.8	35

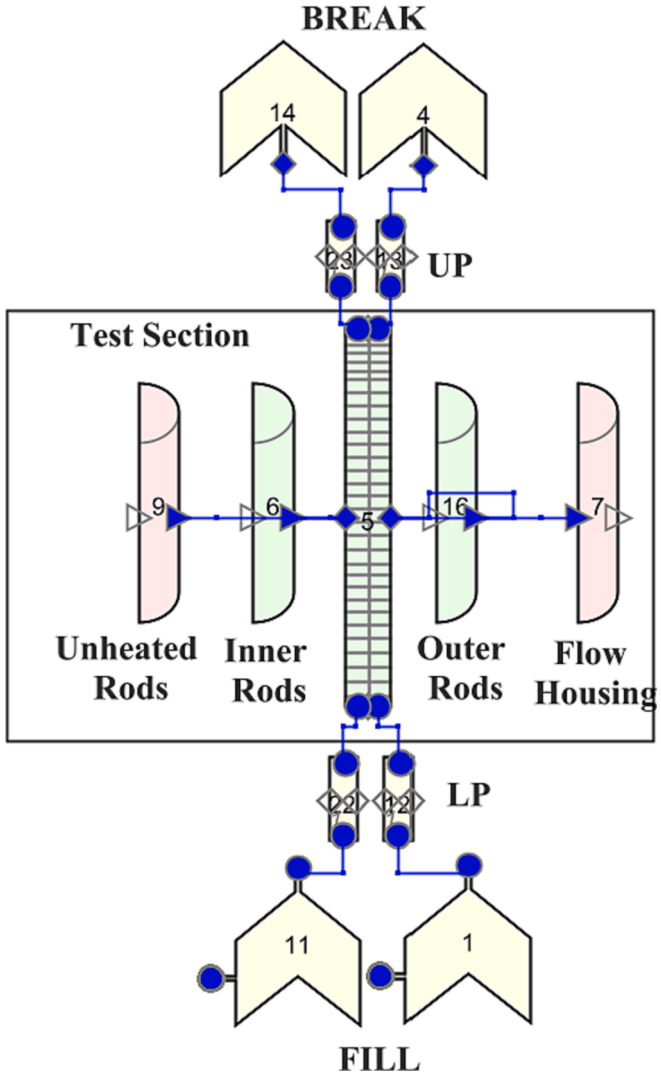

Fig. 6. TRACE nodalization view of the RBHT facility.

2. TRACE droplet field model

Recently, Bernard and Bajorek (2023) modified TRACE code from two-field (TRACE v5p7) to three-field (TRACE 3F) by implementing droplet field and its associated closure relations. This work is significantly enhancing the predictive capability of TRACE in reflood transients. They considered three interfacial source terms, which are droplet size changes due to phase change, film entrainment and pool entrainment. They assessed the performance of the new TRACE 3F capabilities by comparing the results of TRACE v5p7 and TRACE 3F against experimental data obtained from the FLECH-SEASET experimental facility (Hochreiter, 1985). The assessment results revealed a remarkable enhancement in the prediction of the quench front propagation for the low and medium reflood tests. This improvement partially rectified a consistent issue of under-predicting the quench time in TRACE v5.0p7. Both codes, TRACE 3F and TRACE v5.0p7, demonstrated accurate predictions of the peak cladding temperature (PCT), with an overall average deviation of 3 % from the experimental data for all locations below 3.048 m, and the error rise to around 20 % for locations above 3.084 m (Bernard and Bajorek, 2023). Nevertheless, experimental investigations based on RBHT results showed that the spacer grid droplet breakup has noticeable impact on the rod surface temperature, specially in the upper half for the fuel bundle. In this work, TRACE 3F is further modified by introducing another interfacial area source term which account for the droplet breakup from spacer grids (TRACE 3F-DB). Thus, the four interfacial source terms are modeled as

$$\phi_D = \phi_{evap} + \phi_{film} + \phi_{pool} + \phi_{breakup} \tag{1}$$

All of these source terms are associated with mass transfer. This implies that we can connect the mass source to an area source by defining a characteristic diameter through the following relationship:

$$\phi_{generic} = \frac{S_{generic}}{\rho_l D_{characteristic}} \tag{2}$$

More details about the new three field implementation, and the phase change, film entrainment and pool entrainment can be found in (Bernard and Bajorek, 2023). In the current work, the focus will be on the spacer grid droplet breakup.

2.1. Spacer grid droplet breakup model

Spacer grids have a significant influence on the thermal–hydraulic performance of fuel assemblies under both normal and abnormal conditions, as highlighted in references (Cho et al., 2007; Ergun et al., 2008; Koszela, 1998; Miller, 2012). During the reflood phase, the DFFB regime occurs, and heat transfer occurs through various mechanisms, including convection between the heating surface and the vapor phase, interfacial convection between vapor and liquid droplets, radiation heat exchange between the heating surface and the vapor/droplets, as well as direct heat transfer between the heating surface and liquid droplets. Fig. 4 illustrates the breakup process when the incoming droplet collide with the spacer grid.

Typically, incoming droplets divide into two groups based on diameter: a group of large droplets with a similar diameter to the incoming droplets and another group consisting of significantly smaller diameter droplets (Yao et al., 1988). Many researchers have proposed empirical correlations for predicting the Sauter mean diameter of secondary droplets. In their experimental study, Yao et al. (Yao et al., 1988) explored into the phenomenon of water droplet breakup. It was revealed that the diameter of dispersed droplets downstream of a dry spacer grid is depending on the Weber number of the incoming droplets and the spacer grid blockage ratio (S. Lee et al., 1984; Yao et al., 1988). The authors estimated the Sauter mean diameter of the newly formed droplets as follows:

$$\frac{d_{s,32}}{d_o} = A\, We_d^{-B} \tag{3}$$

where We_d is the Weber number of the incoming droplet. Yao et al. (Yao et al., 1988) proposed a method in which A and B are functions of the incoming droplet diameter and width of spacer strap. In contrast, Paik et al. (Paik et al., 1985) utilized constant values for A and B, setting them at 6.16 and 0.53, respectively. The Weber number is defined as the ratio of droplet inertia to surface tension, as indicated in Equation 4.

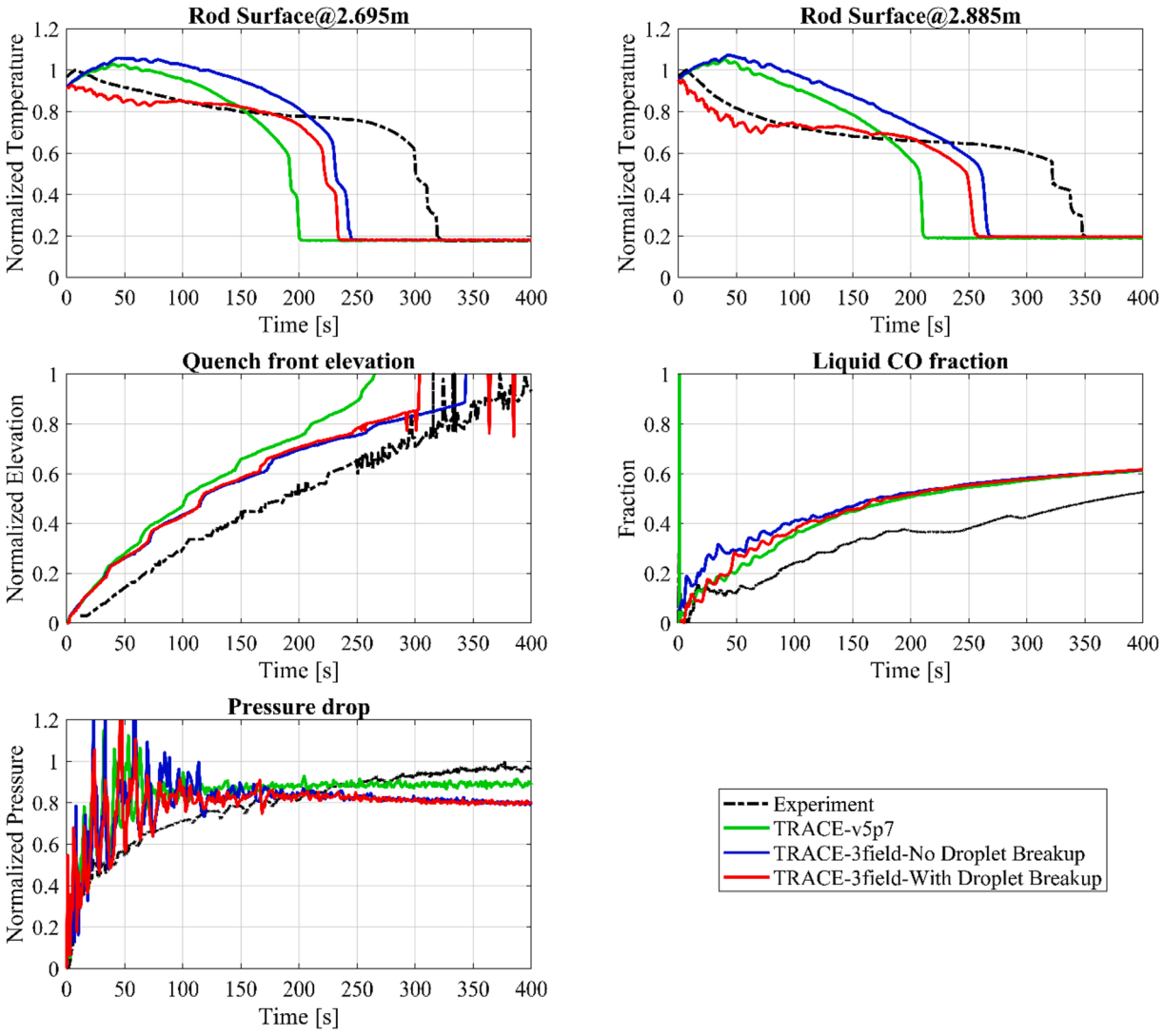

Fig. 7. Evolution of RBHT thermal hydraulic parameters during reflood test −9005.

Consequently, droplets must possess adequate inertial forces ($We_d > We_{crit}$) to undergo the breakup process.

$$We_d = \frac{\rho_d U_d^2 d_o}{\sigma} \tag{4}$$

In their experimental investigation of high Weber number droplets impacting on a heated surface, Akhtar and Yule (Akhtar and Yule, 2001) ntroduced the following empirical correlation for estimating the Sauter mean diameter of secondary droplets:

$$\frac{d_{s,32}}{d_o} = 0.2 + \left(\frac{60}{We_d}\right)^a \quad 1.0 < a < 1.5 \tag{5}$$

Hamdan et al. (Hamdan et al., 2015) conducted a comparison of their experimental findings with the model developed by Yao et al. (Yao et al., 1988), which had been implemented into COBRA-TF code. It was observed that the model resulted in an overestimation of their experimental data. Consequently, they introduced a new modified droplet breakup model specifically designed for droplets with We_d values exceeding 30, as follows:

$$\frac{d_{s,32}}{d_o} = (1.25 - 2.9\exp(-0.09We_d))\left(We_d^{0.8} exp\left(\frac{-78}{We_d}\right)\right)^{-1/3} \tag{6}$$

The previously mentioned models are straightforward approaches for predicting droplet breakup. However, Jin et al. (Jin et al., 2019) demonstrated that the models proposed by Yao et al. (Yao et al., 1988), Lee et al. (S. Lee et al., 1984), and Paik et al. (Paik et al., 1985) consistently underestimated the experimental data for RBHT (Rod Bundle Heat Transfer) with dry spacer grids. In response, the authors extended the original work of Cheung and Bajorek (Cheung and Bajorek, 2011) to enhance the droplet breakup model specifically for dry spacer grids, based on the RBHT experimental data. Their model considers several factors, including the Weber number, spacer grid blockage ratio, kinetic energy and Reynolds number of incoming droplets, interfacial heat transfer, non-dimensional radiation number, distance from the initial breakup point, and the liquid mass loss coefficient due to small droplet evaporation. Accordingly, the Sauter mean diameter of the newly formed droplets downstream of the dry spacer grid can be expressed as:

$$\frac{d_{32}}{d_o} = \frac{1 - \gamma\varepsilon n_s \frac{d_s^3}{d_0^3}}{1 - \gamma\varepsilon n_s \frac{d_s^2}{d_0^2} + \frac{\varepsilon k We_d}{12}} \tag{7}$$

All parameters of Equation 7 have been defined in Table 1. The selected droplet breakup model effectively captures the observed enhancement in interfacial heat transfer, as evidenced by experimental data. This model is applicable to both mixing vane and egg-crate style spacer grids. The spacer grids only partially block the core flow area, and

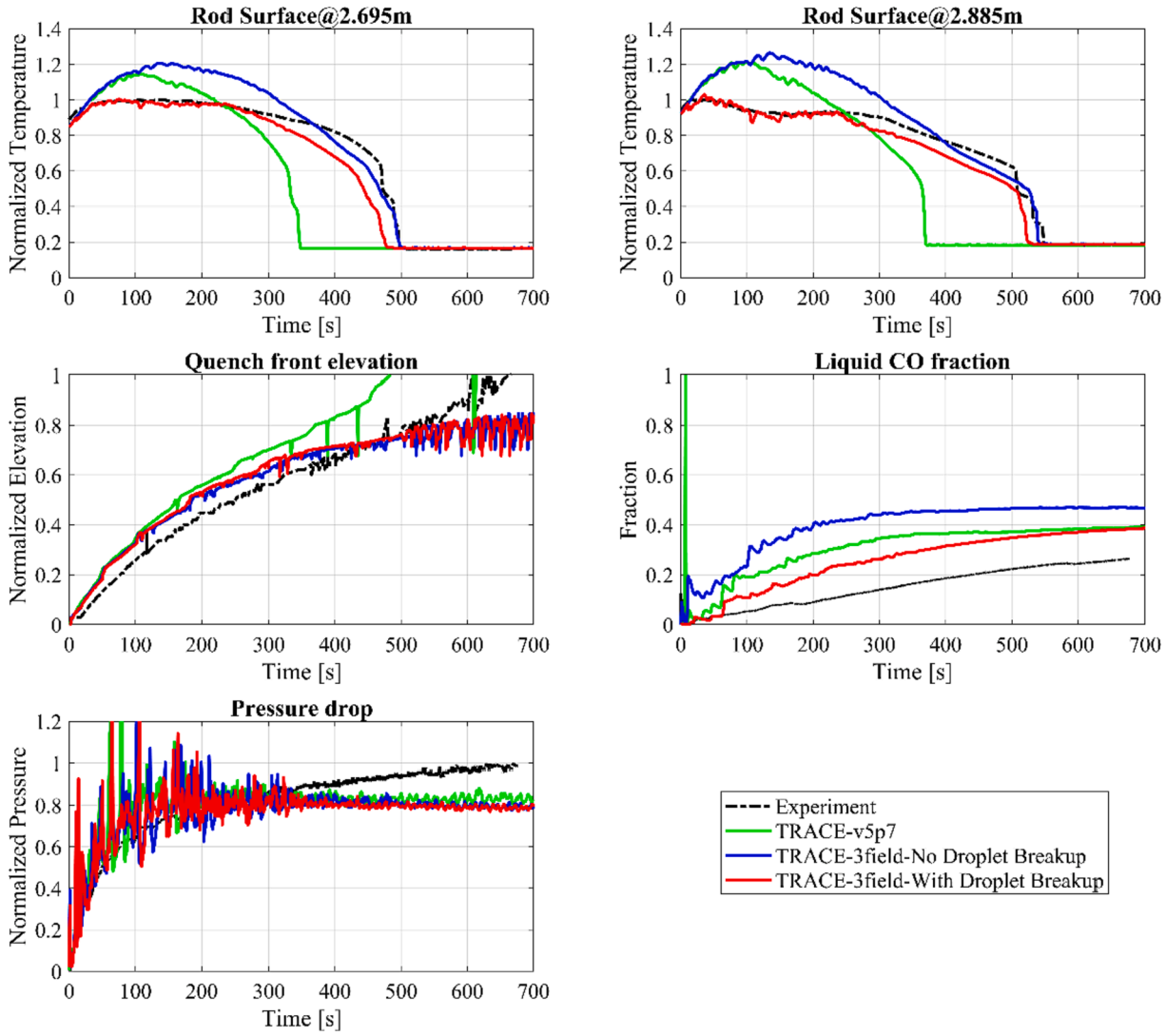

Fig. 8. Evolution of RBHT thermal hydraulic parameters during reflood test −9021.

many of the incoming droplets pass through the spacer grid without any contact with the spacer strap. Thus, the number of droplets colliding with the spacer grid is directly proportional to the spacer grid's blockage ratio, and approximately 60 % of these colliding droplets will undergo breakup (Cheung and Bajorek, 2011). As a result, the mass flow rates of the newly formed small droplets ($\dot{m}_s$) and the unaffected large droplets ($\dot{m}_l$) downstream of the spacer grids can be estimated using Equation 5 and Equation 6, respectively.

$$\dot{m}_s = 0.6\varepsilon \times \dot{m}_o \tag{6}$$

$$\dot{m}_l = \dot{m}_o - \dot{m}_s \tag{7}$$

where ε is the total blockage ratio of the spacer grid and $\dot{m}_0$ is the mass flow rate upstream.

3. TRACE 3F-DB assessment

3.1. RBHT experimental facility

RBHT stands for the Rod Bundle Heat Transfer facility, a dedicated test facility situated at Pennsylvania State University in the United States. Its primary purpose is to explore the behavior of reflood transients within a rod bundle equipped with a spacer grid. The RBHT facility encompasses a 4 m height stainless steel test section, housing a 7 × 7 rod bundle configuration. In addition to the rod bundle, it has both lower and upper plenums, an injection pump, a steam separator, a pressure oscillation damping tank, a boiler, and liquid carryover tanks, as illustrated in Fig. 5 (Lowery et al., 2023).

The rod bundle within this setup simulates a segment of a standard Pressurized Water Reactor (PWR) fuel assembly. In this representation, each rod has a diameter of 9.49 mm, and they are arranged with a rod pitch of 12.59 mm. A total of 45 rods are electrically heated, following a triangular axial power distribution. The power peaks at 150 % of the average power level at a height of 2.74 m within the assembly. Notably, the four rods positioned at the corners remain unheated. The cumulative heated length of the rod bundle spans 3660 mm. The test section is enclosed by an Inconel 600 square flow housing, featuring six transparent windows to observe two-phase flow and droplet behavior throughout the bundle. Furthermore, within the test section, seven mixing vane spacer grids are installed (Jin et al., 2019; Jin et al., 2020).

The RBHT facility has comprehensive instrumentation, totaling 512 data channels, dedicated to capturing critical transient reflood parameters. Within the test section, numerous of temperature (256 TCs) and pressure sensors (23) are strategically positioned to monitor rod surface temperatures, bulk temperature, pressure differentials, and high-speed camera to estimate bubble and droplet sizes. These measurements are required for investigating the quenching behavior during the reflood process. In addition, the facility utilizes two carryover tanks, one small

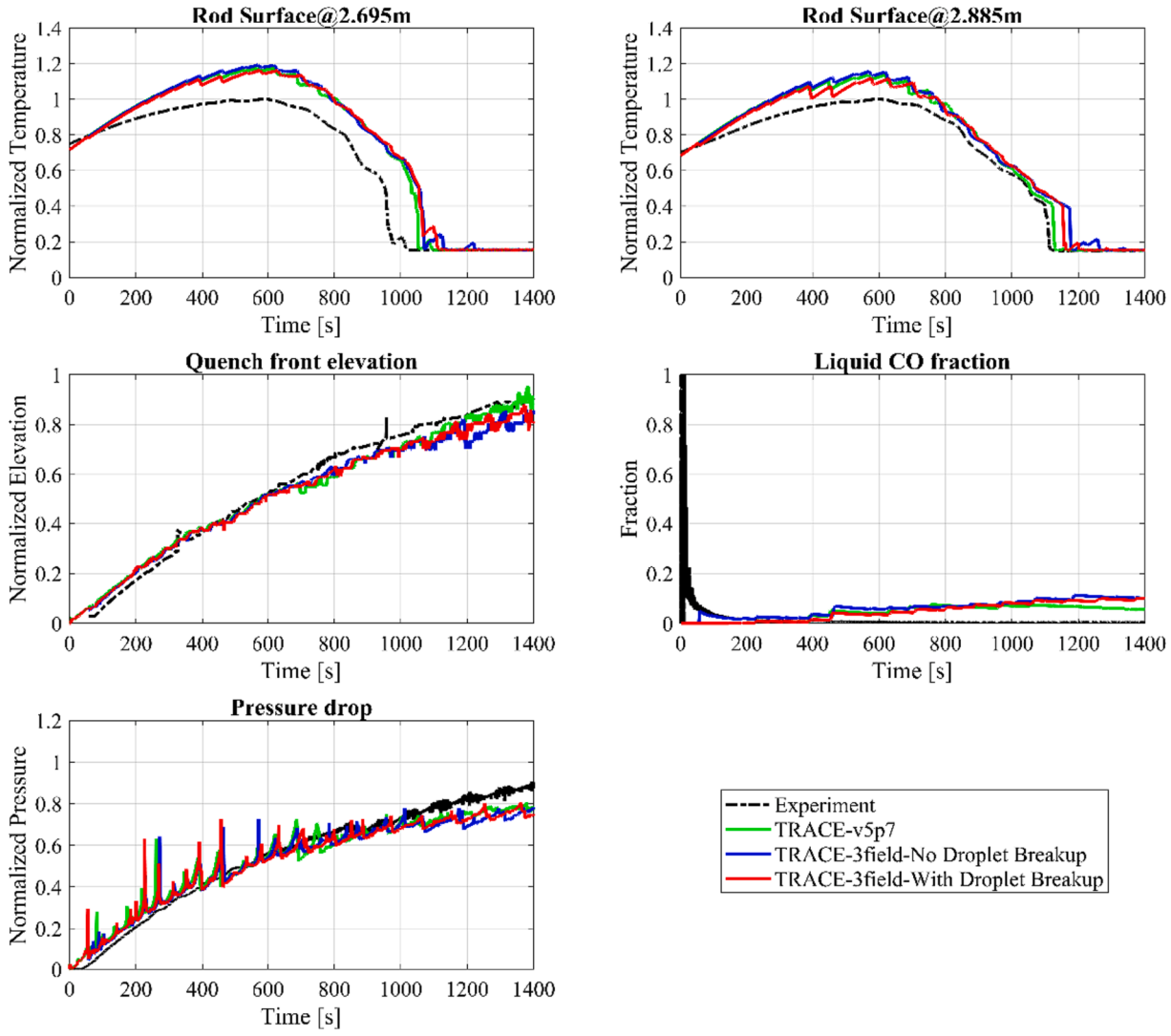

Fig. 9. Evolution of RBHT thermal hydraulic parameters during reflood test −9043.

and one large, to quantify the fraction of liquid carried over during the reflood phase. For a more extensive overview of the RBHT facility, a detailed description can be found in (Hochreiter et al., 2010; Hochreiter et al., 2012; Jin, 2019).

At the beginning of each test, the rod bundle is heated to a specific peak cladding temperature exceeding the Leidenfrost point, corresponding accident scenarios encountered in Light Water Reactors (LWRs). Subsequently, subcooled water, at varying temperatures and mass flow rates, is injected through the lower plenum to initiate the quenching process within the rod bundle. During this quenching phase, a substantial quantity of droplets is generated as the quench front rises through the rod bundle. Numerous RBHT experiments have been conducted, encompassing a wide range of initial and boundary conditions, including varying inlet temperature, inlet flow velocity, operating pressure, and heating power. More recently, as part of the OECD/NEA RBHT project spanning from 2020 to 2022 (OECD/NEA, 2019), eleven open-phase tests were made available to project partners for the evaluation of different system thermal hydraulic codes. In Table 2, you can find a summary of the boundary conditions pertaining to these 11 OECD/NEA RBHT tests (Lowery et al., 2023).

3.2. RBHT TRACE input model

RBHT tests have been extensively employed to validate the thermal hydraulics code TRACE by the US-NRC (Hochreiter et al., 2010; Hochreiter et al., 2012; Jin, 2019; Perret et al., 2019). The RBHT model utilized in this paper is based on the one referred to as 'Trace-v5p5′ in (Perret et al., 2019). In this paper, simulations were conducted using the same TRACE model for the RBHT facility, but with different TRACE versions, TRACE v5.0 patch 7 (v5p7), the newly developed 3-field TRACE, both with and without the droplet breakup model. The model includes various thermal hydraulic and heat structure components, illustrated in Fig. 6. The test section is represented as a 3D Cartesian VESSEL component, with 32, 2, and 1 cells in the axial, Y, and X directions, respectively. The axial cells have varying heights, ranging from 11 cm to 15 cm, except for the initial 10 cm, which is divided into two sections, and above 3.4 m, where it is approximately 9 cm. The two transverse cells (Y) correspond to the flow patterns around two distinct groups of rods: an inner group of 25 heated rods and an outer group comprising 20 heated rods and 4 structural rods. This differentiation is made because these two groups experience slightly different flow conditions due to wall effects from the flow housing. Both heated and unheated rods are simulated using heat structure components, each incorporating 30 axial cells. The test section walls are similarly modeled with heat structure components employing 32 axial cells.

The heated rods, HTSTR6 and HTSTR16, are equipped with 30 axial cells and 9 radial nodes. These rods feature functionalities such as liquid level tracking, axial conduction, and a fine mesh reflood model, all

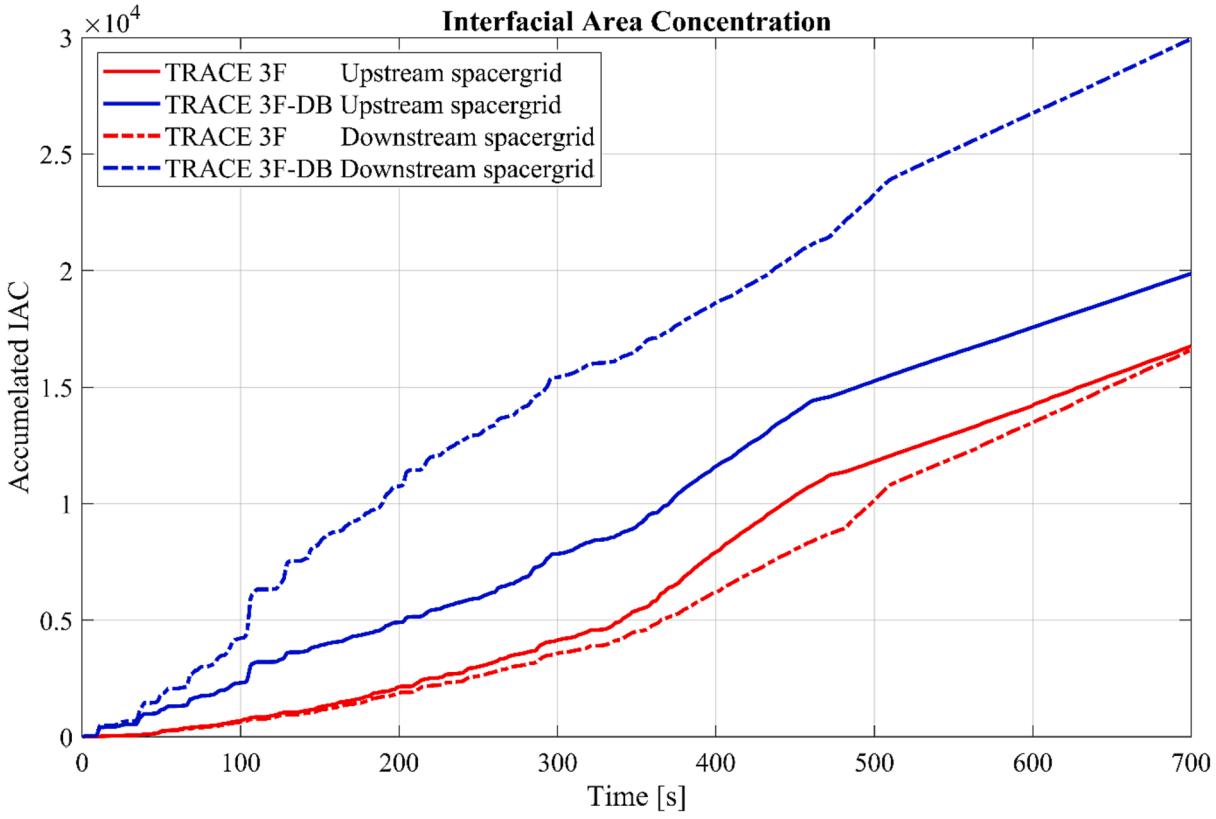

Fig. 10. The influence of spacer grid droplet breakup on the Interfacial Area Concentration (IAC) during reflood test 9021.

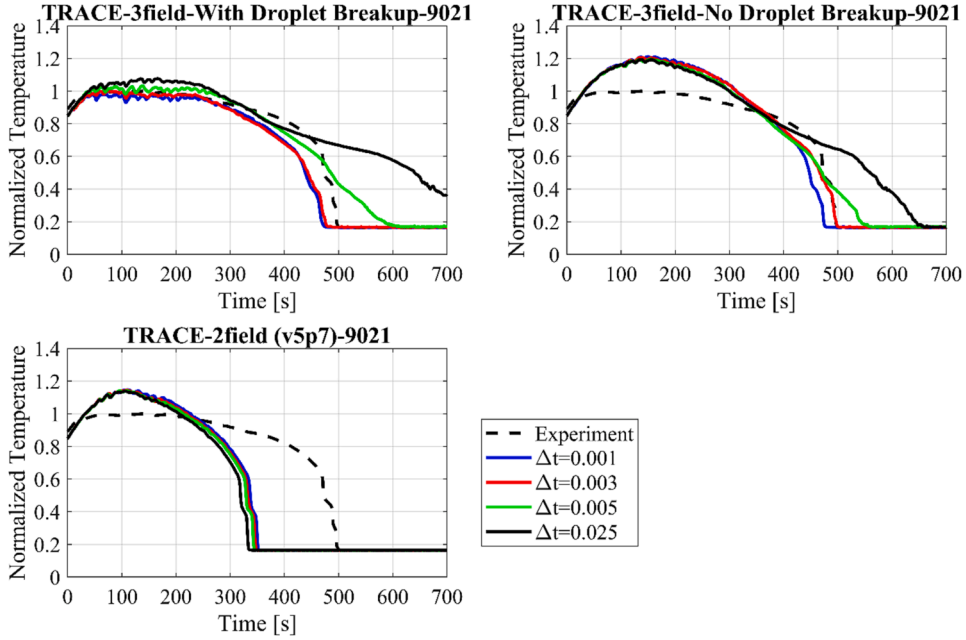

Fig. 11. RBHT rod surface temperature at 2.695 m for low reflood rate and low subcooling temperature case (2.5 cm/s, and 10 K).

enabled. Since there is no heating in the top two cells of the VESSEL, only 30 axial cells are incorporated into the rod heat structures. The distribution of power within the heated rods is provided by a POWER component. In contrast, the flow housing (HTSTR7) consists of 32 axial cells and 3 radial nodes, with axial conduction enabled. However, it lacks fine meshes, and neither liquid level tracking nor the reflood model is enabled for this heat structure. This heat structure is not powered, and no consideration is given to heat loss from the outer surface of the flow housing. The heat structure associated with the structural corner rods (HTSTR9) includes 30 axial cells and 5 radial nodes, with axial conduction and liquid level tracking functionalities enabled. Similar to the flow housing, fine meshes are removed, and the reflood model is not activated for this heat structure.

As shown in Fig. 6, there are two inlet boundary conditions (FILL)

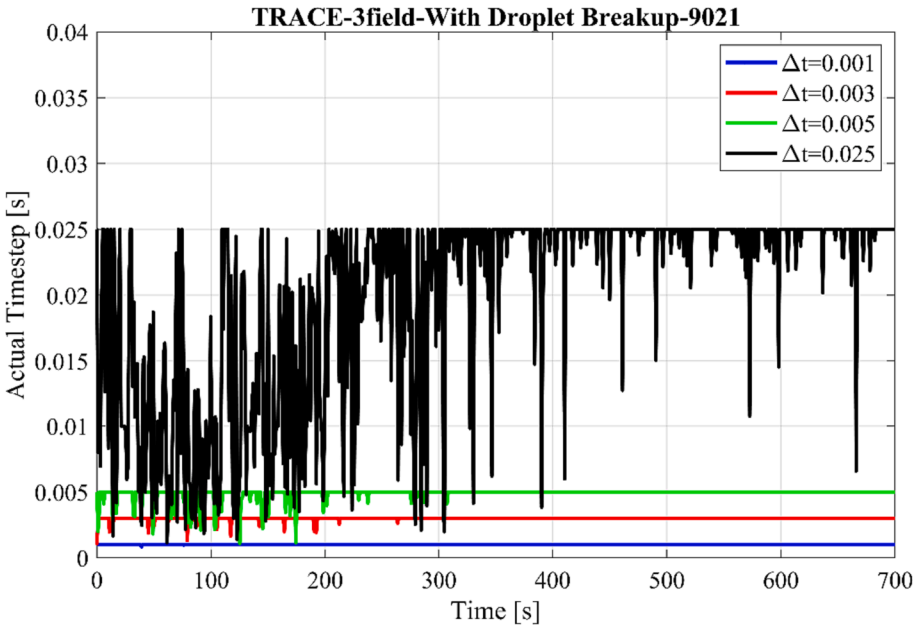

Fig. 12. The actual TRACE 3F-DB selected time step for low reflood case 9021.

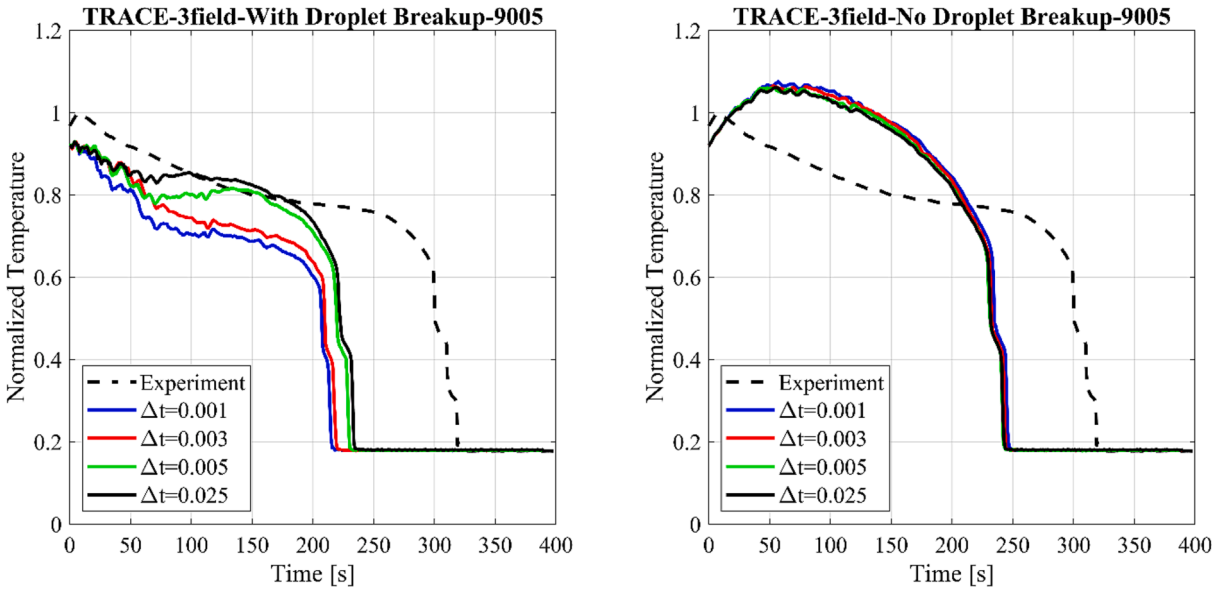

Fig. 13. RBHT rod surface temperature at 2.695 m for medium reflood rate and low subcooling temperature case (5.0 cm/s, and 10 K).

and two outlet boundary conditions (BREAK) components connected to two pipes. These pipes are linked to the inlet and outlet regions of the VESSEL component. The hydraulic diameter and flow area of these pipes are designed to correspond with those of the inner and outer regions of the vessel. Regarding the outlet (BREAK) components, they are initially set with pressure and mixture temperature values derived from the experimental system pressure. In contrast, the inlet (FILL) components are configured with initial pressure and temperature values determined based on the experimental subcooling temperature.

4. Results and discussion

4.1. Spacer grid effect on rod surface temperature

In general, spacer grids play a crucial role in influencing the flow dynamics within the fuel assembly, particularly in scenarios involving two-phase flows. In this section, we will investigate how the spacer grid droplet breakup model affects the accuracy of predicting reflood phenomena. To do this, we will compare the predicted outcomes generated by three different simulations: TRACE v5p7, a three-field TRACE simulation without considering droplet breakup (3F), and a three-field TRACE simulation incorporating droplet breakup (3F-DB). These predictions will be compared against experimental data from the RBHT facility, utilizing the same TRACE model throughout all tests. The initial boundary conditions for these simulations were derived from the experimental data at the beginning of the tests. The results of specific tests are presented in Fig. 7 to Fig. 12.

Beginning with test 9005, which features an inlet velocity of 5 cm/s, inlet subcooling of 10 K, and peak power of 1.31 kW/m, the general pattern of rod surface temperature at two distinct axial positions (2.695 m and 2.885 m from the inlet) is comparable across all three simulations. Nevertheless, the maximum rod surface temperature and quenching

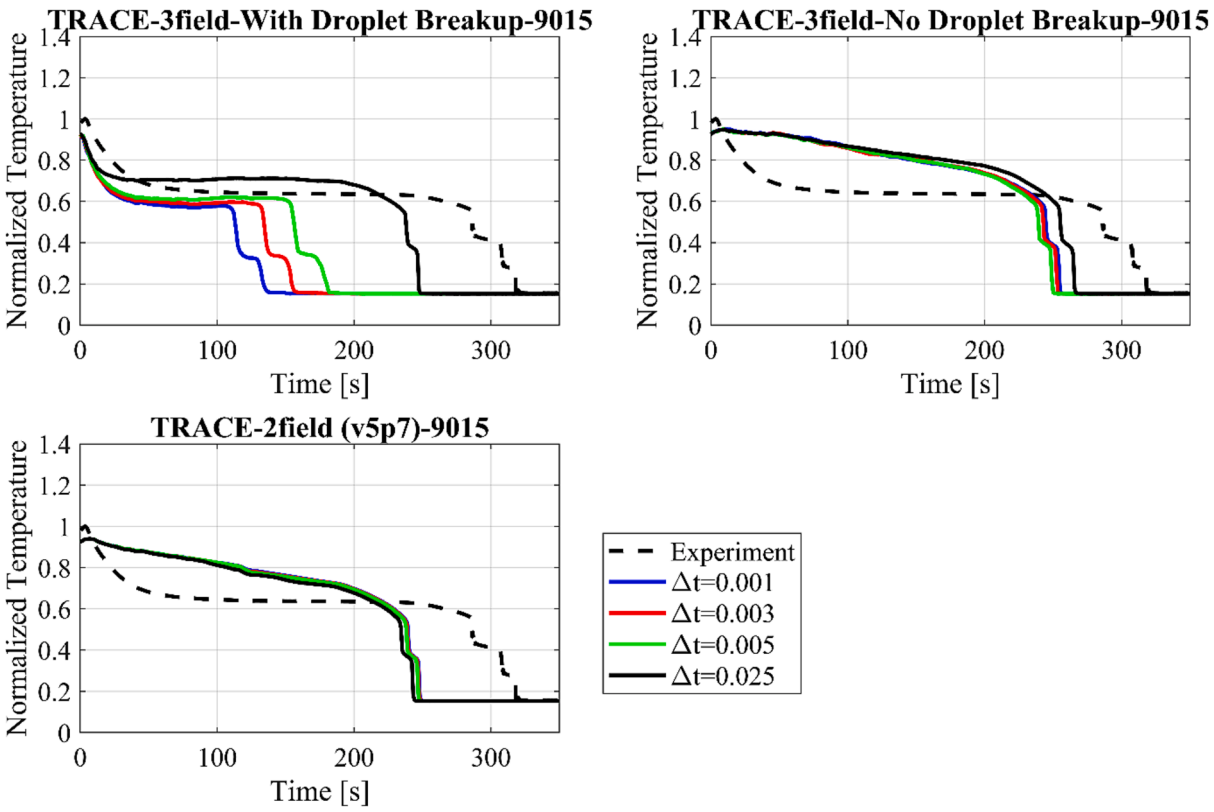

Fig. 14. RBHT rod surface temperature at 2.695 m for high reflood rate and low subcooling temperature case (15.0 cm/s, and 10 K).

time are different, as shown in Fig. 7. Before reaching the quenching phase, both TRACE v5p7 and TRACE 3F tend to overestimate rod surface temperatures, while TRACE 3F-DB demonstrates better predictive accuracy. Corresponding to the experimental data, TRACE 3F-DB exhibits a rapid decrease in rod surface temperature at the initial stages of the test. In contrast, TRACE v5p7 and 3F simulations show an initial temperature rise lasting for the first 50 s, followed by a gradual decrease. These discrepancies in the calculations primarily appear from the influence of droplet field and droplet breakup models, which enhance interfacial heat and mass transfer. Additionally, the simulations indicate an earlier quenching of the rods compared to the experimental results. Notably, both TRACE 3F and 3F-DB offer more accurate estimates of quenching time than TRACE v5p7, with a difference of approximately 50 s. However, there is an overprediction of the liquid carryover fraction after approximately 25 s from the start of the test. In contrast, TRACE v5p7 and 3F-DB provide slightly better estimates of liquid carryover during the initial 100 s. Furthermore, the total pressure drop is initially overestimated for the first 150 s, followed by underestimation. This trend is influenced by the average void fraction and quench elevation.

As illustrated in Fig. 8, the above observed trend is replicated in test 9021. This test operates at a lower reflood rate, featuring an inlet velocity of 2.5 cm/s and maintaining the same peak power as test 9005. Due to the reduced reflood rate, the quenching process experiences a delay. In test 9021, the difference between TRACE v5p7 results and the experimental data becomes more pronounced. However, TRACE 3F-DB successfully predicts the rod surface temperatures at 2.695 m and 2.885 m accurately. In terms of quenching time, both TRACE 3F and 3F-DB provide precise predictions, whereas TRACE v5p7 initiates quenching approximately 150 s earlier across the entire test section. Furthermore, at the upper part of the test section, TRACE 3F and 3F-DB calculations indicate a delay in quenching, with no occurrence near the outlet. Additionally, all versions of TRACE tend to overestimate the liquid carryover fraction.

Fig. 9 displays the experimental and calculated results of test 9043, which explores a scenario characterized by an extremely low reflood rate. In this experiment, an inlet velocity of 0.5 cm/s and a peak power of 0.32 kW/m are applied. Within the first half of the test section, all three simulations provide a reasonably accurate depiction of the quenching front, although a delay of approximately 20 s is observed in the upper part of the test section. This discrepancy accounts for the slight underestimation of pressure drop by the TRACE model in the later stages of the test. Over the first 600 s of the experiment, the temperature of the rod surface gradually rises, reaching a peak 20 % higher than its initial temperature, followed by a gradual reduction until the rod bundle experiences quenching. For all TRACE calculations, the maximum rod surface temperature consistently is around 20 % higher than the experimental data at a position of 2.695 m and approximately 10 % higher at 2.885 m, as depicted in Fig. 9. This figure illustrates that the calculated rod surface temperature remains consistent across all three versions of TRACE. This suggests that, during scenarios involving very low reflood rates, the droplet field has a negligible impact, or the generated droplets are sufficiently small to be captured using the existing single-group droplet field model.

As interpreted through various reflood tests, the thermal hydraulic dynamics of the reflood scenario are strongly influenced by the specific conditions during reflood. The implementation of a droplet field in TRACE significantly enhances its predictive capabilities for reflood transients. Moreover, the phenomenon of droplet breakup has a substantial impact on heat and mass transfer within the rod bundle. The breakup results in many smaller-diameter droplets, thereby raising the interfacial area concentration (IAC). As shown in Fig. 10, TRACE 3F-DB estimates a higher total IAC compared to TRACE 3F. As estimated, the IAC in TRACE 3F-DB substantially increases downstream of the spacer grid due to droplet breakup. In contrast, TRACE 3F exhibits a slightly reduced IAC downstream of the spacer grid, representing an unrealistic behavior. This discrepancy is further highlighted in Fig. 2, where the temperature downstream of the spacer grid is lower than upstream, attributed to the increased IAC resulting from droplet breakup through

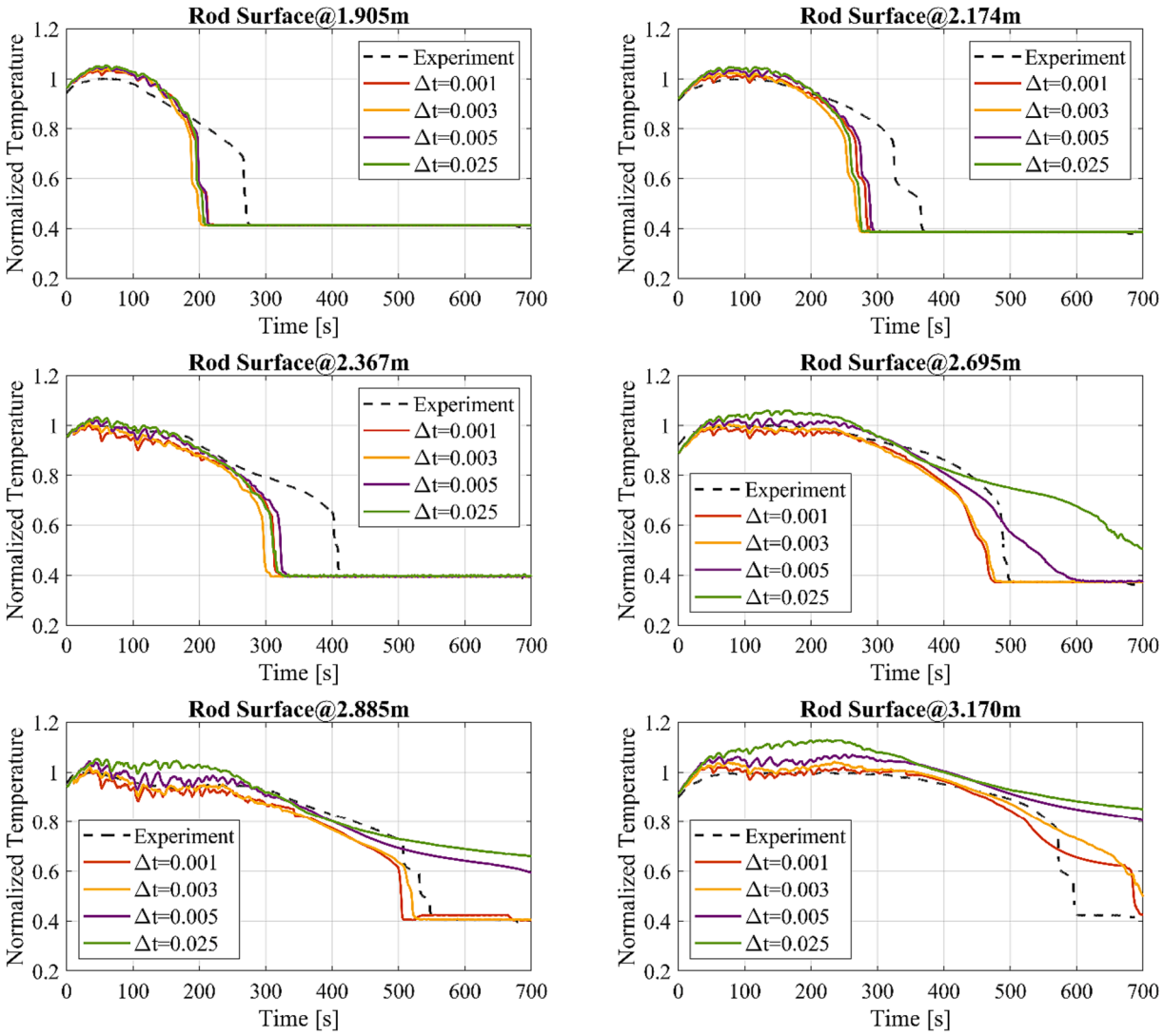

Fig. 15. Influence of time step on the axial temperature distribution for test 9021 (2.5 cm/s, and 10 K).

the spacer grid, as verified by TRACE code results.

4.2. *Time step effect on the reflood prediction*

In this section, we conduct a sensitivity analysis to examine the impact of varying the time step on the prediction of rod surface temperature and quenching time during the reflood process. Our simulations utilize TRACE 3F and TRACE 3F-DB to model RBHT tests mentioned in Table 2, employing four different maximum time step values: 0.001, 0.003, 0.005, and 0.025 s. The simulations consistently employ the same TRACE model.

The outcomes of this sensitivity analysis are illustrated in Fig. 11 to Fig. 14, where we compare TRACE's predictions of rod surface temperature against experimental measurements. Our findings reveal that increasing the time step leads to a delay in the quenching time, with this effect being particularly noticeable under conditions of low reflood rates and low subcooling temperatures. The sensitivity of these operational conditions to the time step is noteworthy, as even a slight adjustment from 0.003 to 0.005 s can result in a substantial change of the quenching time, up to 100 s. In contrast, an increase in the time step to 0.025 s leads to unrealistic behavior in both rod surface temperature and quenching time, although the TRACE code continues to run without crashing. It is worth noting that the time step does not exert a significant influence on the predictions of peak cladding temperature (PCT) for case 9021. The TRACE code employs a semi-implicit numerical scheme, with the time step automatically adjusted to ensure that the Courant number remains less than or equal to one. However, if the maximum input time step meets the Courant limitation, TRACE utilizes this maximum time step for calculations. If the maximum time step fails to satisfy the Courant limitation, the time steps are accordingly reduced. In the case of 9021, where the reflood rate is relatively low at 2.5 cm/s, TRACE requires small time steps to meet the Courant number condition. As illustrated in Fig. 12, TRACE decreased the time step to less than 0.004 s during the initial 200 s. Consequently, the time step does not significantly influence the PCT for this case. In all cases, the time step does not have influence on the results of the two-field TRACE v5p7, which indicates that the dispersed droplets have a large impact on the numerical system behavior. This also can explain the variations between TRACE 3F and TRACE 3F-DB results, in which the later creates larger number of droplets with smaller diameters.

Under experimental conditions with a medium reflood rate of 5.0 cm/s and a low subcooling temperature of 10 K, as seen in the case of 9005, Fig. 13 demonstrates that the numerical time step has a negligible impact on the results obtained through TRACE 3F. Nevertheless, when we increase the time step for TRACE 3F-DB, we observe a rise in the peak cladding temperature (PCT). However, this increase in PCT only leads to a slight delay of approximately 10 s in the quenching time when transitioning from a time step of 0.001 to 0.025 s. On the other hand, for

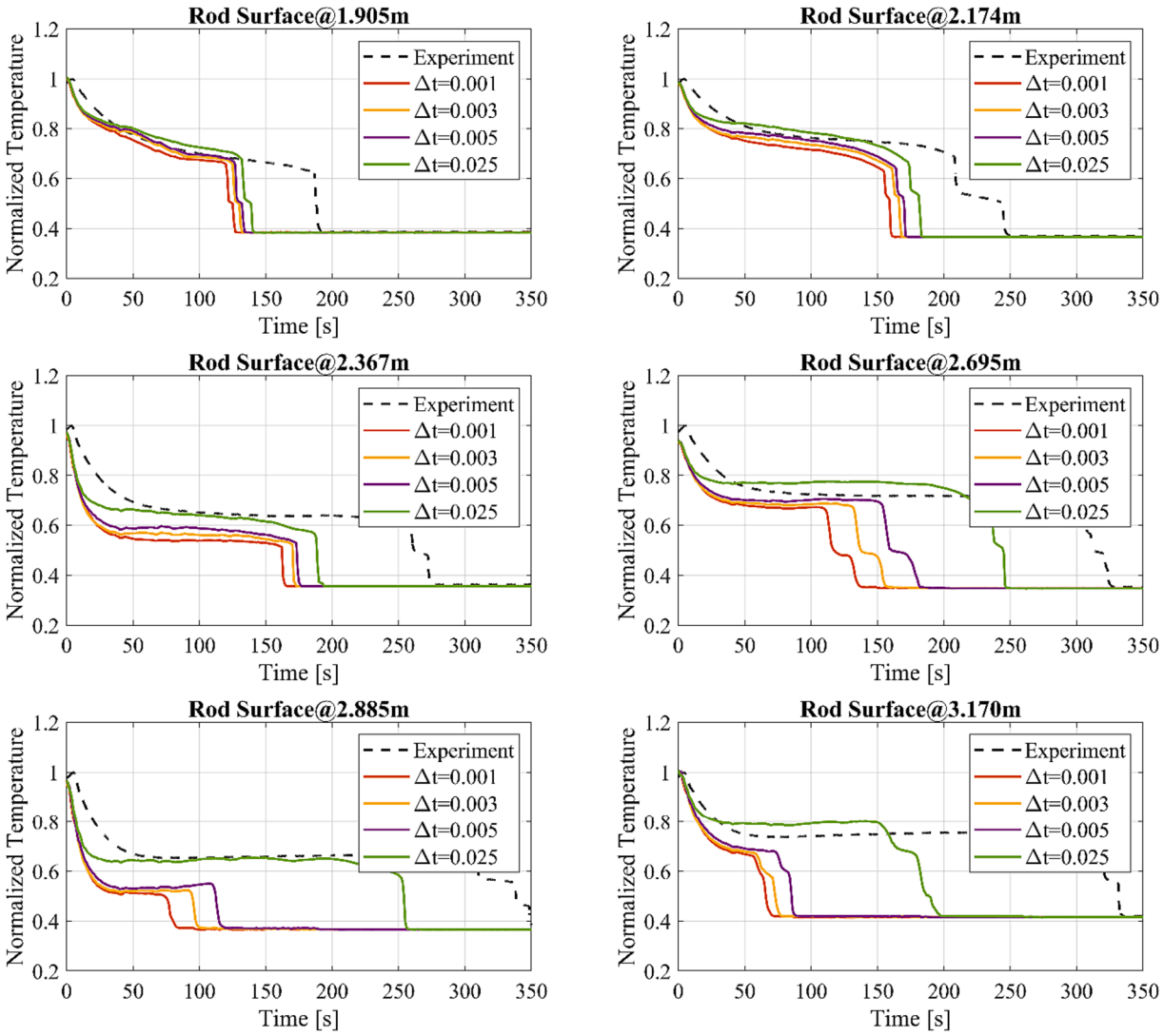

Fig. 16. Influence of time step on the axial temperature distribution for test 9015(15.0 cm/s, and 10 K).

high reflood rates, such as 15 cm/s, and low subcooling temperatures of 10 K, as described in case 9015, the time step significantly influences the predictions of PCT and quenching time, as illustrated in Fig. 14. The results obtained using TRACE v5p7 and TRACE 3F remain relatively stable despite variations in the time step. These two code's versions lack to the physical modeling of droplet field and droplet breakup, respectively. Since the droplet field properties have the largest impact of the system behavior, the influence of time step appears more in the TRACE 3F-DB.

The RBHT simulations have shown that the effect of the time step depends on the reflood rate and subcooling temperature. However, this effect becomes particularly evident in the second half of the heated length, specifically downstream of the power peak location, as shown in Fig. 15 to Fig. 16. In this region, the complexity of the two-phase flow increases, and both the droplet field and droplet breakup become more sensitive to changes in the time step. This sensitivity is most pronounced for high reflood rates and low subcooling temperatures, as represented in Fig. 16 for the 9015 case. The influence of the time step is minimal for low reflood rates and high subcooling temperatures.

In general, system analysis codes are designed to simulate and model a wide range of physical phenomena through large thermal hydraulic systems within a reasonable calculation time. These codes typically use best estimate methods and include various assumptions to represent the complex thermal hydraulic system in a simple 1D and/or 3D models. Therefore, several source of errors can be found during the validation process, such as lack of physical representation, spatial and/or time steps, convergence criteria, and input specifications. Generally, the cell size and time step are related to each other. However, the cell size must satisfy the ($L/D_h \geq 10$) conditions, whereas the axial length should me around 10 times larger than the hydraulic diameter (U.S.NRC, 2022). In this study, 32 axial nodes have been used to model the RBHT fuel assembly, which is approximately at the limitation boundary ($L/D_h \approx 10$). Therefore, the sensitivity analysis has been performed on the time step size. TRACE code utilizes the semi-implicit numerical scheme, and the time step can be automatically adjusted to satisfy Courant number to be less than or equal one. However, large time steps amplify the numerical truncation errors, and reducing time step leads to increase the numerical diffusion. To understand the numerical diffusion, consider the revised expression for truncation error after substituting the Tayler series expansions into the original finite volume equation (Hirt, 1968; U.S.NRC, 2022):

$$\left.\frac{\partial \rho}{\partial t}\right|_i^n + \left.\frac{\partial \rho}{\partial x}\right|_i^n = \frac{V}{2}(\Delta x - V\Delta t)\left.\frac{\partial^2 \rho}{\partial x^2}\right|_i^n + O(\Delta x^2, \Delta t^2) \quad (1)$$

where ρ is the density for the mass conservation equation, V is the velocity, Δx is the spatial distance, and Δt is the time step. This equation (1) is a standard advection–diffusion equations with a diffusion coeffi-

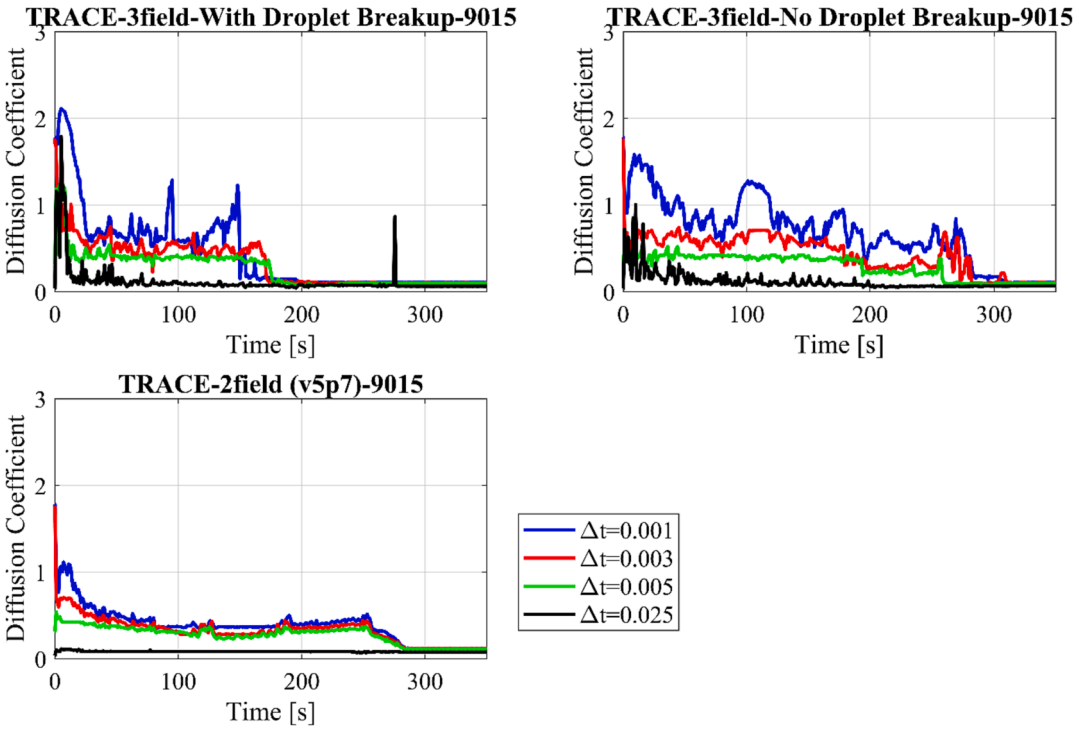

Fig. 17. Numerical diffusion at different time steps.

cient of:

$$D = \frac{V}{2}(\Delta x - V\Delta t) \quad (2)$$

For stable solution, the diffusion coefficient must be greater than zero, in which the time step should be small enough to satisfy the conditions in equation (2). However, it needs to be close to zero for accurate solution. The diffusion coefficient depends on the fluid velocity (liquid, droplet, and gas). Therefore, understanding the physical phenomena through the simulated system is very important for best estimate analysis. For illustration, the best estimated TRACE 3F-DB results for case 9015 have obtained at 0.025 s as maximum time step, and as shown in Fig. 17, the numerical diffusion is the lowest for time step of 0.025 s. This analysis can provide a guidelines for modeling and simulations using system analysis codes.

5. Conclusion

This paper introduced a novel droplet field capability for TRACE code. The closure relationships for the droplet field from existing literature and TRACE v5.0p7′s closure models were utilized into TRACE 3F. The droplet breakup model is implemented into TRACE 3F as source term for the interfacial area transport. The new modified TRACE code was referred as TRACE 3F-DB. This study assessed the performance of three different versions of TRACE (v5p7, 3F, and 3F-DB) in their ability to predict the reflooding transient during LOCA scenarios. The assessment was based on experimental tests conducted at RBHT, which involved varying reflood rates and inlet velocities. It was observed that spacer grids had a significant impact on the flow dynamics within the fuel assembly, particularly when dealing with two-phase flow scenarios. This study further investigated the impact of incorporating spacer grid droplet breakup models on the prediction of reflooding phenomena. The findings highlighted that the models incorporating droplet field and droplet breakup mechanisms substantially improved the heat and mass transfer at the interfaces. Consequently, the inclusion of a droplet breakup model was key role for enhancing prediction accuracy in simulations of reflood phenomena. TRACE 3F and 3F-DB were found to offer better predictions compared to TRACE v5p7, particularly in terms of quenching time and rod surface temperatures. However, it was noted that all TRACE models tended to overestimate the liquid carryover fraction. Additionally, during scenarios with very low reflood rates, the influence of the droplet field was minimal, possibly due to the small size of the generated droplets, which could not be accurately captured by the current single-group droplet field model.

Furthermore, a sensitivity analysis conducted in this study emphasized the significant impact of the time step on predicting rod surface temperature and quenching time during reflooding, especially in cases involving low reflood rates and low subcooling temperatures. Increasing the time step led to delays in quenching time, and even a slight adjustment could produce significant changes in quenching time. However, increasing the time step beyond a certain threshold resulted in unrealistic behavior in rod surface temperature and quenching time predictions. The effect of the time step was less pronounced in predicting peak cladding temperatures in some cases, although in others, a slight increase in the time step led to higher peak cladding temperatures. The time step's influence was most notable in the second half of the heated length, downstream of the power peak location, where the complexities of two-phase flow, droplet field, and droplet breakup were more sensitive to variations in the time step. However, for scenarios with low reflood rates and high subcooling temperatures, the influence of the time step was minimal. In conclusion, selecting an appropriate time step was essential for accurate predictions of rod surface temperature and quenching time during reflood simulations. Accurate modeling of the reflooding process in both BWRs and PWRs was emphasized as essential for ensuring the safety of nuclear power plants.

The new three-field TRACE version utilizes single entrained droplet field. Nevertheless, within the flow channel, various sizes of entrained droplets max exist, particularly during droplet breakup. The single droplet filed assumption maintains the overall concentration of the interfacial area. Consequently, the newly developed TRACE 3F-DB version accurately predicts the rod surface temperature and quenching front. However, single droplet approach influences the precision of drag and energy calculations. Therefore, further research could explore the impact of multi-droplet field of the enhancement of the pressure drop

and carryover predictions. Additionally, TRACE uses the thermal equilibrium assumption for the droplet and continues liquid. Thus, a separate energy equations for the continuous liquid and droplet filed will be considered in the future works.

CRediT authorship contribution statement

Omar S. Al-Yahia: . **Matthew Bernard:** Conceptualization, Investigation, Methodology, Resources, Writing – original draft, Data curation, Software. **Ivor Clifford:** Project administration, Resources, Supervision, Writing – original draft, Writing – review & editing, Data curation, Funding acquisition. **Gregory Perret:** . **Stephen Bajorek:** Funding acquisition, Project administration, Resources, Software, Supervision. **Hakim Ferroukhi:** Funding acquisition, Project administration, Resources, Supervision.

Declaration of competing interest

The authors declare that they have no known competing financial interests or personal relationships that could have appeared to influence the work reported in this paper.

Data availability

Data will be made available on request.

Acknowledgment

This work was funded by the Swiss Nuclear Safety Inspectorate ENSI (CTR00604) within the framework of the STARS program (http://www.psi.ch/stars).

References

Akhtar, S., Yule, A., 2001. Droplet impaction on a heated surface at high Weber numbers. ILASS-Europe, Zurich, p. 37.

Bernard, M., & Bajorek, S. M. (2023, August 20–25, 2023). *Implementation of a Three-Field Framework in TRACE to Improve the Prediction of Reactor Core Reflood Conditions Part I* 20th International Topical Meeting on Nuclear Reactor Thermal Hydraulics (NURETH-20), Washington, D.C.

Cheung, F.B., Bajorek, S.M., 2011. Dynamics of droplet breakup through a grid spacer in a rod bundle. Nucl. Eng. Des. 241 (1), 236–244. https://doi.org/10.1016/j.nucengdes.2010.10.017.

Chiou, J., Hochreiter, L., Utton, D., & Young, M. (1982). Spacer grid heat transfer effects during reflood. Joint NRC/ANS Meeting on Basic Thermal Hydraulic Mechanisms in LWR Analysis.

Cho, S., Moon, S.-K., Chun, S.-Y., Kim, Y.-S., Baek, W.-P., 2007. Spacer grid effects during a reflood in an annulus flow channel. J. Nucl. Sci. Technol. 44 (7), 967–976.

Choi, T.S., No, H.C., 2010. Improvement of the reflood model of RELAP5/MOD3.3 based on the assessments against FLECHT-SEASET tests. Nucl. Eng. Des. 240 (4), 832–841. https://doi.org/10.1016/j.nucengdes.2009.11.043.

Choi, T.S., No, H.C., 2012. An improved RELAP5/MOD3.3 reflood model considering the effect of spacer grids. Nucl. Eng. Des. 250, 613–625. https://doi.org/10.1016/j.nucengdes.2012.06.025.

Chun, T.-H., Oh, D.-S., 1998. A pressure drop model for spacer grids with and without flow mixing vanes. J. Nucl. Sci. Technol. 35 (7), 508–510.

Ergun, S., Hochreiter, L.E., Mahaffy, J.H., 2008. Modifications to COBRA-TF to model dispersed flow film boiling with two flow, four field Eulerian-Eulerian approach – Part 2. Ann. Nucl. Energy 35 (9), 1671–1676. https://doi.org/10.1016/j.anucene.2008.02.014.

Hamdan, K.S., Kim, D.-E., Moon, S.-K., 2015. Droplets behavior impacting on a hot surface above the Leidenfrost temperature. Ann. Nucl. Energy 80, 338–347. https://doi.org/10.1016/j.anucene.2015.02.021.

Hirt, C.W., 1968. Heuristic stability theory for finite-difference equations. J. Comput. Phys. 2 (4), 339–355.

Hochreiter, L., Cheung, F., Lin, T., Frepoli, C., Sridharan, A., Todd, D., Rosal, E., 2010. Rod bundle heat transfer test facility test plan and design. NUREG CR-6975. US Nuclear Regulatory Commission.

Hochreiter, L., Cheung, F., Lin, T., Spring, J., Ergun, S., Sridharan, A., Ireland, A., & Rosal, E. (2012). *RBHT reflood heat transfer experiments data and analysis. University Park (PA): US Nuclear Regulatory Commission; 2012*.

Hochreiter, L. (1985). *FLECHT SEASET program. Final report*.

IAEA. (2003). Safety margins of operating reactors, Analysis of uncertainties and implications for decision making V. International Atomic Energy Agency.

In, W.-K., Chun, T.-H., Shin, C.-H., Oh, D.-S., 2008. Numerical computation of heat transfer enhancement of a PWR rod bundle with mixing vane spacers. Nucl. Technol. 161 (1), 69–79.

Ishii, M., Hibiki, T., 2010. Thermo-fluid dynamics of two-phase flow. Springer Science & Business Media.

Jin, Y., 2019. Investigation of Two-Phase Flow Thermal-Hydraulic Behavior in Rod Bundle during Reflood Transients Based on the RBHT Experimental Data. The Pennsylvania State University.

Jin, Y., Cheung, F.-B., Shirvan, K., Bajorek, S.M., Tien, K., Hoxie, C.L., 2019. Development of a droplet breakup model for dry spacer grid in the dispersed flow film boiling regime during reflood transients. Int. J. Heat Mass Transf. 143, 118544 https://doi.org/10.1016/j.ijheatmasstransfer.2019.118544.

Jin, Y., Cheung, F.-B., Shirvan, K., Bajorek, S.M., Tien, K., Hoxie, C.L., 2020. Development of a new spacer grid pressure drop model in rod bundle for the post-dryout two-phase flow regime during reflood transients. Nucl. Eng. Des. 368, 110815.

Koszela, Z., 1998. Effects of spacer grids with mixing promoters on reflood heat transfer in a PWR LOCA. Nucl. Technol. 123 (2), 156–165.

Koszela, Z., 2003. Assessment of RELAP5/MOD3.2.2 Gamma against ABB Atom 3×3-Rod Bundle Reflooding Tests. Nucl. Eng. Des. 223 (1), 49–73. https://doi.org/10.1016/S0029-5493(03)00004-9.

Lee, S., Cho, S., Rob, K., Sheen, H., & Aghili, M. (1983). *LDA in situ study of droplet hydrodynamics across grid spacers in PWR-LOCA reflood*.

Lee, S., Sheen, H., Cho, S., & Issapour, I. (1984). *Measurement of droplet dynamics across grid spacer in mist cooling of subchannel of PWR*.

Lee, S. L., Cho, S., & Sheen, H. (1984). *A study of droplet hydrodynamics across a grid spacer*. Division of Accident Evaluation, Office of Nuclear Regulatory Research, US ….

Lowery, B. R., Hanson, M. K., Garrett, G. R., Miller, D. J., Almudhhi, T., Cheung, F. B., Bajorek, S. M., Tien, K., & Hoxie, C. L. (2023, August 20–25, 2023). *Reflood Thermal-Hydraulics Testing Using the NRC-PSU Rod Bundle Heat Transfer (RBHT) Test Facility* 20th International Topical Meeting on Nuclear Reactor Thermal Hydraulics (NURETH-20), Washington, D.C.

Miller, D. J. (2012). Single-phase and two-phase grid-enhancement heat transfer in the reflood stage of a loss of coolant accident.

Nithianandan, C., Klingenfus, J., & Reilly, S. (1995). *RELAP5 model to simulate the thermal-hydraulic effects of grid spacers and cladding rupture during reflood*.

OECD/NEA. (2019). *Rod Bundle Heat transfer (RBHT) Project*. https://www.oecd-nea.org/jcms/pl_25253/rod-bundle-heat-transfer-rbht-project.

OECD/NEA. (2022). *RBHT Project Report*.

Paddock, M.D., 1977. Axial Photographic Technique for Droplet Size and Distribution of Two-Phase Dispersed-Annular Flow Through a Simulated. Nuclear Reactor Grid Wichita State University.

Paik, C., Hochreiter, L., Kelly, J., & Kohrt, R. (1985). *Analysis of FLECHT-SEASET 163-rod blocked bundle data using COBRA-TF*.

Pederson, C.O., 1967. The Dynamics and Heat Transfer Characteristics of Water Droplets ImpingingUpona Heated Surface. Carnegie Mellon University.

Perret, G., Clifford, I., & Ferroukhi, H. (2019, March 6-11, 2022). *Bias and uncertainty considerations for trace predictions of RBHT reflood experiments* 19th international topical meeting on nuclear reactor thermal hydraulics (NURETH-19), Brussels.

Rane, A., Yao, S., 1981. Turbulent mist flow heat transfer in straight ducts. ASME J. Heat Transfer 103, 679–684.

Senda, J., 1982. Experimental studies on the behavior of a small droplet impinging upon a hot surface. ICLASS- 82, 397.

Sugimoto, J., Muraov, Y., 1984. Effect of grid spacers on reflood heat transfer in PWR-LOCA. J. Nucl. Sci. Technol. 21 (2), 103–114.

U.s.nrc., 2022. TRACE V5.0 Patch 7 Theory Manual. Office of Nuclear Regulatory Research.

Wachters, L.H.J., Westerling, N.A.J., 1966. The heat transfer from a hot wall to impinging water drops in the spheroidal state. Chem. Eng. Sci. 21 (11), 1047–1056. https://doi.org/10.1016/0009-2509(66)85100-X.

Yao, S., Hochreiter, L., & Cai, K. (1988). Dynamics of droplets impacting on thin heated strips.